http://dx.doi.org/10.5012/bkcs.2011.32.10.3629

The Effect of a Sol-gel Formed TiO_2 Blocking Layer on the Efficiency of Dye-sensitized Solar Cells

Tae-Yeon Cho,[†,‡] Soon-Gil Yoon,[‡] S. S. Sekhon,[§] Man Gu Kang,[#] and Chi-Hwan Han[†,*]

[†]*Photovoltaic Research Center, Korea Institute of Energy Research, Daejeon 305-343, Korea. [*]E-mail: hanchi@kier.re.kr*
[‡]*Department of Material Science and Engineering, Chung-Nam National University, Daeduk Science Town 305-764, Korea*
[§]*Department of Physics, Guru Nanak Dev University, Amritsar-143005, India*
[#]*Ionic Device Team, IT-NT Group, Electronics and Telecommunications Research Institute, Daejeon 305-700, Korea*
Received June 10, 2011, Accepted August 10, 2011

The effect of a dense TiO_2 blocking layer prepared using the sol-gel method on the performance of dye-sensitized solar cells was studied. The blocking layer formed directly on the working electrode, separated it from the electrolyte, and prevented the back transfer of electrons from the electrode to the electrolyte. The dye-sensitized solar cells were prepared with a working electrode of fluorine-doped tin oxide glass coated with a blocking layer of dense TiO_2, a dye-attached mesoporous TiO_2 film, and a nano-gel electrolyte, and a counter electrode of Pt-deposited FTO glass. The gel processing conditions and heat treatment temperature for blocking layer formation affected the morphology and performance of the cells, and their optimal values were determined. The introduction of the blocking layer increased the conversion efficiency of the cell by 7.37% for the cell without a blocking layer to 8.55% for the cell with a dense TiO_2 blocking layer, under standard illumination conditions. The short-circuit current density (J_{sc}) and open-circuit voltage (V_{oc}) also were increased by the addition of a dense TiO_2 blocking layer.

Key Words : Dye-sensitized solar cell, Photo anode, Blocking layer, Sol-Gel method, High efficiency

Introduction

Dye-sensitized solar cells (DSCs) have attracted much attention over the last decade, due to their low production cost and potentially high conversion efficiency.[1-3] A typical working electrode of a DSC is generally composed of a dye-attached mesoporous TiO_2 film coated on a transparent conductive oxide (TCO) glass. A platinized conductive glass is used as a counter electrode, and an electrolyte containing an I^-/I_3^- redox couple is used to fill in between the two electrodes. A typical DSC is comprised of a TCO-coated glass/dye-attached TiO_2 layer/electrolyte/platinized counter electrode. A large number of dye molecules encasing the large surface area of TiO_2 nanoparticles enables efficient light harvesting. However, electron/charge transport is a limiting factor in the performance of the electron-collecting layer of the nano-particles.

Upon light irradiation, dye photosensitizers adsorbed onto the surface of a wide band gap TiO_2 semiconductor readily inject electrons into the conduction band of the solid.[4] The electron injection is a very fast process that occurs in a femto second time frame. In the absence of an electrolyte, the electron back transfer takes place more slowly, typically in a microsecond/millisecond time frame.[5] This charge recombination process can be intercepted by the reaction of a reducing mediator (I^-/I_3^-) with the oxidized dye. Thus, the overall efficiency of the light-induced charge separation depends on the kinetic competition between the back electron transfer and the dye regeneration processes. The oxidized dye must be regenerated by reducing the mediator to prevent back electron transfer from the TiO_2 semiconductors. DSCs have proved to be very efficient at exploiting this principle. In this system, the I^-/I_3^- redox mediator travels back and forth by diffusion between the two electrodes, to shuttle to the sensitizer the electrons that have gone through the electrical circuit. The rate of the reaction between the oxidized dyes and iodide, following charge injection, is crucial for the efficiency of the energy conversion device. The faster the reaction rate, the more electrons are forced to leave the semiconductor, contributing to the photocurrent.

A back electron transfer can also take place between the TCO and the electrolyte. The injected electrons from the dyes are collected into the TCO *via* the mesoporous film of TiO_2 nanoparticles, which occurs at a much higher rate than the back transfer to the dye and electrolyte, as described above. However, the electrons collected at the TCO can also be back-transferred to the electrolyte by the reaction of an oxidized mediator of I_3^-, as the electrolyte is in contact with TCO through the mesoporous TiO_2 film. This may reduce the photocurrent and the overall conversion efficiency of DSC.

Unidirectional flow of charge with no electron leakage at the interfaces is very critical for the high-energy conversion efficiency of DSCs. In general, there are 4 important interfaces: transparent conducting oxide (TCO)/TiO_2; TiO_2/dye; dye/electrolyte; and electrode/counter electrode that play an important role in the overall performance of DSCs.[6] The details of different interfacial mechanisms and the plan that can be used to improve the performance of DSCs by employing interface-engineering principles have recently been

reviewed in detail.[7] Previously, 4-tert butylpyridine was added to the electrolyte to decrease the carrier leakage of the direct electron acceptance from the TiO_2 electrode. As this method is not very effective, TiO_2 film has recently been introduced as a blocking layer between the TCO and the porous film in the DSC.[8] The blocking layer prevents direct physical contact between the TCO and the electrolyte, and has been reported to lead to an increase in the overall conversion efficiency of the cell. The charge recombination is a common process in DSCs, which limits their performance and mainly takes place at the TiO_2/sensitizer and TCO/TiO_2 interfaces.[9] The kinetic features of the charge transfer processes in DSCs demonstrate that charge recombination at the TiO_2/sensitizer interface is negligible. The charge recombination at the TCO/TiO_2 interface occurs due to the physical contact between the electrolyte and the TCO surface. Due to the mesoporous structure of the TiO_2 layer, the electrolyte percolates and electron transfer on the TCO surface becomes possible. However, this can be prevented by introducing a compact oxide layer on the TCO before the TiO_2 mesoporous layer. The blocking layer reduces the reaction of photoinjected electrons and the I_3^- ions at the TCO/electrolyte interface.

In addition to TiO_2,[10,11] blocking layers of Nb_2O_5[12] and insulating polymers,[13] MgO, ZnO, Al_2O_3, Eu_2O_3 and SiO_2,[14] have also been used by different researchers. The effect of preparation of the TiO_2 blocking layer by different methods, such as spray pyrolysis, dip coating, spin coating, sol-gel, chemical vapor deposition, radio-frequency (RF) and reactive direct-current (DC) sputtering, has also been studied with regard to the effect on the performance of DSCs.[9,15]

In the present work, prior to the coating of a mesoporous TiO_2 film on TCO, a dense film of TiO_2 100-500 nm thick was coated directly on the TCO as a blocking layer to physically separate the TCO from the electrolyte. The blocking layer was coated by a screen printing method that used a screen-printable sol prepared by the Pechini sol-gel method. The effects of the gel processing conditions and heat treatment temperature on the morphology of the blocking layer, and their effect on the photovoltaic parameters and cell efficiency, were studied.

Experimental

Preparation of Sol for Blocking Layer Coating. For the processing of coating the blocking layer, a polyester-based titanium sol was prepared by the addition of Ti-isopropoxide into ethylene glycol, followed by heating at 60 °C. A corresponding amount of citric acid (Fluka) was added to the mixture with continuous stirring, followed by heating at 90 °C until the mixture became clear. The molar ratio of the sol was 1:6:24 [$Ti(iOPr)_4$:citric acid:ethylene glycol]. The sol was coated by screen printing onto fluorine-doped tin oxide glass (FTO, TEC 8, 2.3 mm, Pilkington), which was then heat-treated at various temperatures. The as-coated sol was then transformed into a blocking layer of TiO_2. The thickness of the layer ranged from 100 to 500 nm. The formation of the dense oxide layer, microstructure, morphology and thickness of the blocking layer were studied by thermogravimetry/differential thermal analysis (TG/DTA) and scanning electron microscopy (SEM).

Preparation of TiO_2 Photoanodes. A paste of TiO_2 nanoparticles (Ti-20, ENB Korea) was deposited on the conducting glass with a fluorine-doped stannic oxide layer (FTO, TEC 8/2.3 mm, 8 Ω/□, Pilkington) using a screen-printing method. The resulting layer was calcined for 2 h at 550 °C in a muffle furnace. This process was repeated 3 times or until a thickness of 15 μm was obtained. The area of the prepared porous TiO_2 electrode was 25 mm^2 (5 mm × 5 mm). Dye absorption was carried out by dipping the TiO_2 electrode in a 4×10^{-4} M *t*-butanol/acetonitrile (1:1, Merck) solution of standard ruthenium dye: N719 (Solaronix) for 48 h at 25 °C. The photoelectrode was then washed, dried, and immediately used to measure the performance of the solar cell.

Fabrication of DSCs. Transparent counter electrodes were prepared by placing a few drops of 10 mM hydrogen hexachloroplatinate (IV) hydrate (99.9%, Aldrich) in 2-propanol on drilled FTO glass. After calcination at 450 °C for 2 hours, the counter electrode was assembled with the dye-adsorbed TiO_2 photoanode. The two electrodes were separated with 25 μm Surlyn and sealed by heating. The internal space was filled with the electrolyte through drilled holes, which were later sealed with Surlyn and cover glass.

Photovoltaic Characterization. The photo-electrochemical properties of the prepared DSCs were measured using a computer-controlled digital source meter (Potentiostat/Galvanostat Model 273A, EG&G) and a solar simulator (AM 1.5, 100 mW/cm^2, Oriel) as a light source. Photovoltaic performance was characterized by V_{oc}, J_{sc}, and fill factor (FF), and the overall efficiency was characterized by the *J-V* curve. V_{oc} is the electrical potential between the photo-anode and cathode of the solar cell with no external load. J_{sc} is the measured current when the circuit between the photo-anode and cathode has the connection with the least resistance. FF is the ratio of maximum power performance to its ideal maximum power by V_{oc} and J_{sc}. η can be defined as ($V_{oc} \cdot J_{sc} \cdot FF/P_s$), where P_s is the intensity of the incident light.

Results and Discussion

The blocking layer of TiO_2 was prepared using the Pechini sol-gel method.[16] The details of the sol-gel process used for preparation of the TiO_2 blocking layer are shown schematically in Figure 1. The blocking layer was coated onto FTO glass by a screen printing method. The thermal properties of the sol were studied by simultaneous TG/DTA measurements in the 25-700 °C temperature range at a heating rate of 5 °C/minute and TG/DTA plots are shown in Figure 2. The TG plot shows no weight loss up to 100 °C, and above this temperature weight loss took place in multiple steps. The exothermic peaks above 250 and 350 °C are probably generated by the evaporation of excess ethylene glycol and citric acid respectively. The cross linking reaction takes place at

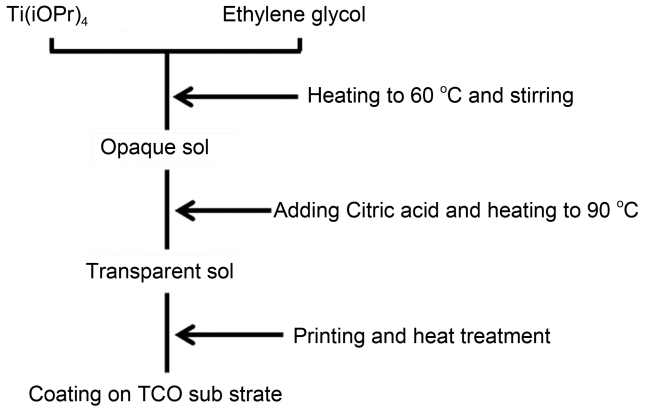

Figure 1. Sol-gel process for dense TiO_2 blocking layer coating using the Pechini method.

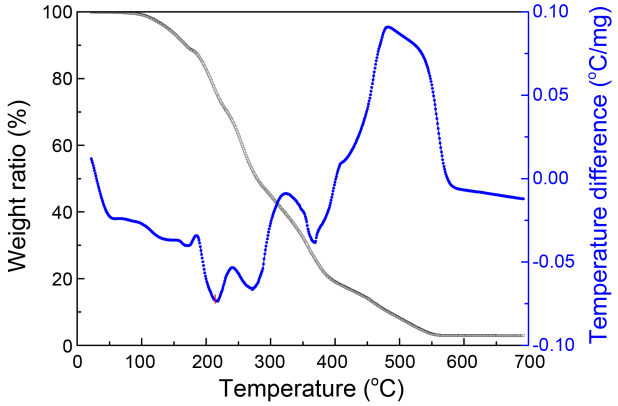

Figure 2. TG and DTA plots of the sol recorded between 30 and 900 °C at a heating rate of 5 °C/min.

500 °C and the peaks at 538 °C can be attributed to the formation of the TiO_2 dense layer.[17] The char weight of around 2-3% at higher temperatures is due to the TiO_2.

The correlation between the heat treatment temperature of the TiO_2 blocking layer and the cell performance was studied in order to optimize the experimental conditions of blocking layer formation for carrier blockage. The temperature for heat treatment was varied from 450 to 600 °C in 4 equal steps. The FTO glass substrate coated with the TiO_2 blocking layer was heat treated at 450, 500, 550 and 600 °C. The surface morphology of the blocking layer was studied by SEM and the micrographs are given in Figure 3. Both the FTO and TiO_2 blocking layers are distinctly visible in the micrographs. Of the 4 samples, the one heat-treated at 550 °C showed the best-consolidated dense TiO_2 layer on FTO glass and homogeneous morphology. The homogeneous and compact morphology of the blocking layer was due to the smaller particle size of the TiO_2 blocking layer prepared by the sol-gel method. The smaller particles can be more efficiently packed on the TCO substrate surface, and as a result the size of the voids present among the particles decreases, which reduces the percolation of the electrolyte.[3] The compact nature of the blocking layer is very essential for its use in DSCs, where it will physically separate the FTO glass from the electrolyte without allowing any percolation of the electrolyte on to the FTO glass.

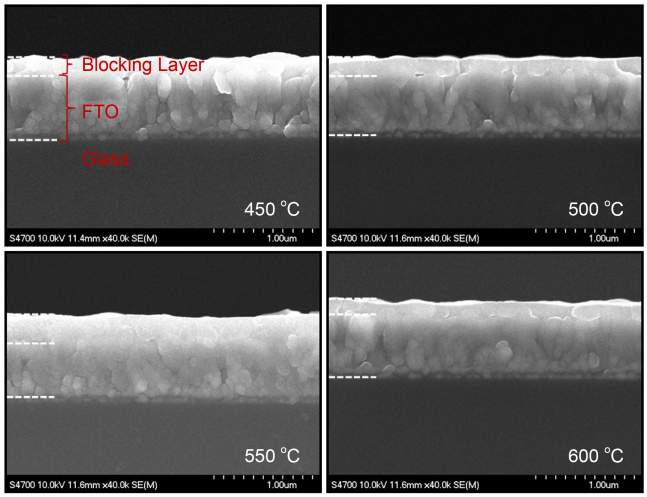

Figure 3. SEM images of the dense TiO_2 on FTO glass heated at various temperatures between 450 and 600 °C.

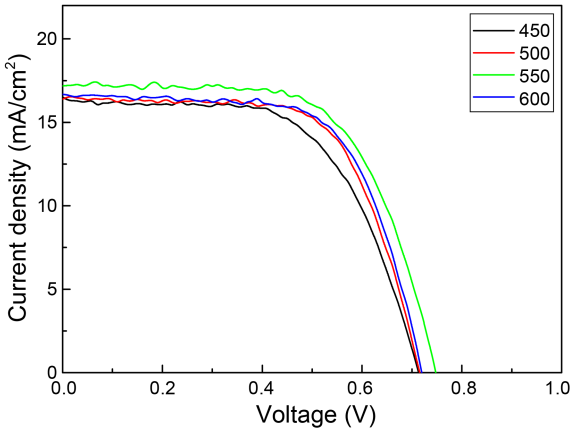

Figure 4. Photocurrent (I) and photovoltage (V) characteristics of DSC using TCO with a blocking layer heated at various temperatures between 450 and 600 °C.

DSCs were assembled using the 4 samples heated at different temperatures, and the photocurrent *vs.* photovoltage characteristics of the cells are given in Figure 4. The different photovoltaic parameters of the DSCs using the TiO_2 blocking layers heat-treated at different temperatures were determined from Figure 4 and are listed in Table 1. The cell using a blocking layer heat-treated at 550 °C showed the best performance. The J_{sc} (17.17 mA/cm^2) and V_{oc} (0.75 V) were observed for this cell. The increase in J_{sc} at higher temperatures is probably due to the improvement of the electron transport characteristics in the TiO_2 blocking layer, and the blocking layer has higher conductivity at higher temperatures, which results in a lower recombination rate for the mobile electrons generated optically at the dye material. The increase in the protective effect against ionic penetration from the electrolyte through the blocking layer results in an enhancement in the V_{oc} value of the cell.[8] The overall cell conversion efficiency was 8.24%, which was 12% higher than for the cell heat-treated at 450 °C, and V_{oc} also showed

Table 1. Photovoltaic parameters of DSCs with TiO_2 sol heat-treated at different temperatures

Temperature (℃)	J_{sc} (mA/cm^2)	V_{oc} (V)	ff	Efficiency (%)
450	16.52	0.71	0.60	7.07
500	16.38	0.72	0.66	7.74
550	17.17	0.75	0.64	8.24
600	16.69	0.72	0.66	7.88

an increase by 40 mV. The increases in J_{sc} and V_{oc} due to a decrease in the recombination rate at the TCO/electrolyte interface are in agreement with the theoretical results.[18,19] The heat treatment temperature of 550 °C was used in further studies.

It was mentioned above that during the preparation of the blocking layer using the sol-gel method shown in Figure 1, after adding citric acid, the sol was heated to 90 °C to obtain a transparent sol. In order to get a higher V_{oc} value, the thickness of the TiO_2 blocking layer should be controlled and optimized. The thickness of the blocking layer was controlled in the present work by varying the reaction time of the sol from 35 to 65 minutes (35, 45, 55 and 65 minutes). It was then heat-treated at 550 °C, which has been found to be the optimum time for the best cell performance (Fig. 4, Table 1). The morphology of the blocking layer prepared by heating the sol for different lengths of time was studied by SEM, and the micrographs are shown in Figure 5. In order to determine the optimum value of the reaction time, DSCs were fabricated using TiO_2 blocking layers with different thicknesses. The thickness of the blocking layer was found to increase from 115 to 321 nm with an increase in the reaction time from 35 to 65 min. The photocurrent *vs.* photovoltage characteristics of the cells are given in Figure 6. For comparison, a cell was also fabricated with no blocking layer. The different photovoltaic parameters of the DSCs using TiO_2 blocking layers with different thicknesses were determined from Figure 6 and are listed in Table 2. The

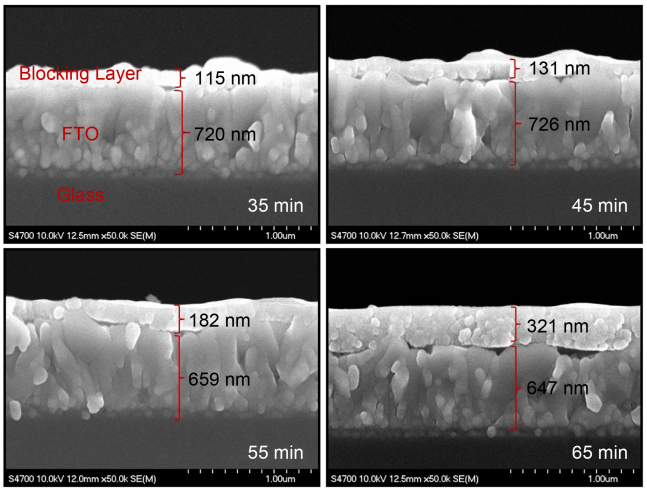

Figure 5. SEM images of the dense TiO_2 on FTO glass heated with various sol reaction times at 90 °C.

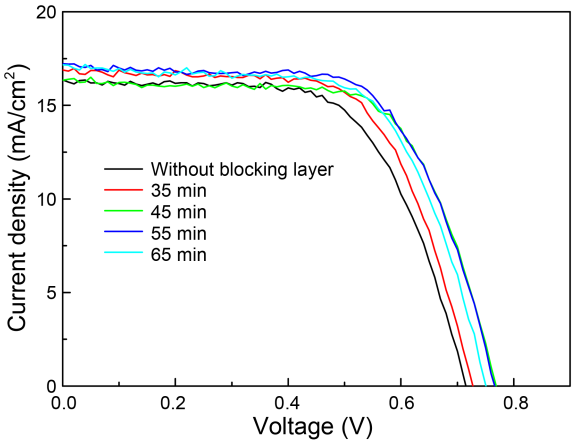

Figure 6. Photocurrent (I) and photovoltage (V) characteristics of DSC using TCO with a blocking layer with different sol reaction times at 90 °C and heat-treated at 550 °C.

Table 2. Photovoltaic parameters of DSCs with TiO_2 sol at different reaction times

Reaction times (min)	J_{sc} (mA/cm^2)	V_{oc} (V)	ff	Efficiency (%)
Without blocking layer	16.36	0.71	0.63	7.37
35	16.88	0.73	0.65	8.02
45	16.34	0.77	0.67	8.42
55	17.23	0.77	0.65	8.55
65	17.16	0.75	0.65	8.37

results in Figure 6 and Table 2 show that the cell in which the sol heating time was 55 minutes (182 nm dense layer) showed the best cell performance. The maximum values of J_{sc} (17.23 mA/cm^2), V_{oc} (0.77 mV) and cell efficiency (8.55%) were obtained for this cell with the blocking layer. The overall cell efficiency was found to increase by 16%, from 7.37% for the cell without a blocking layer to 8.55% for the cell with the TiO_2 blocking layer. Earlier, an increase in cell efficiency from 4.5 to 5.49% has also been reported[20] with the addition of five TiO_2 blocking layers. However, the overall cell efficiency (8.55%) observed in the present case is higher. A 0.87 mA/cm^2 increase in current density and a 60 mV increase in open circuit voltage were also observed in this case. The results obtained in the present study are consistent withThe effect of the dense TiO_2 blocking layer, introduced between the TCO and the TiO_2 electrode, on the resistance of the TCO/TiO_2 interface was also studied by impedance spectroscopy. The impedance plot of DSC with and without the blocking layer was recorded and is given in Figure 7. The radius of the second semicircle, which gives the resistance between the electrode and the electrolyte, was decreased with the introduction of the blocking layer. The decrease in resistance with the introduction of the TiO_2 blocking layer helps with the unidirectional charge transport at the TCO/TiO_2 interface.[6]

The IPCE data for the DSCs with the TiO_2 blocking layer (sol reaction time 55 minutes and heat treatment temperature

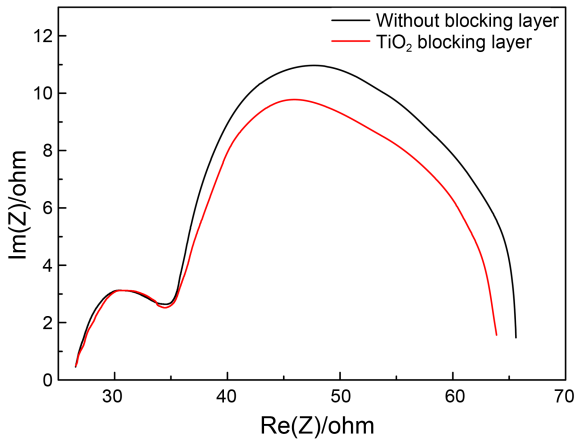

Figure 7. Impedance spectra of DSCs without and with a blocking layer (sol reaction time of 55 min, heat treatment temperature of 550 °C).

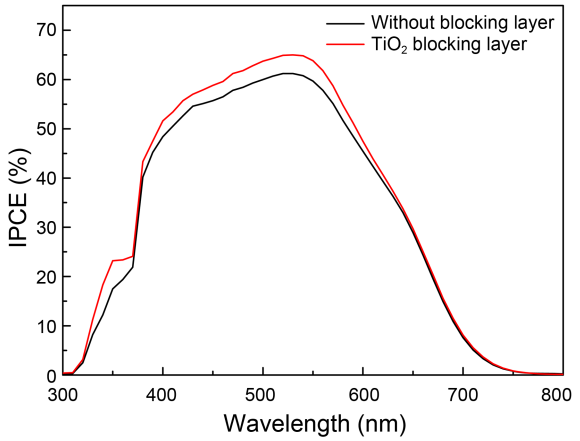

Figure 8. IPCE data of DSCs without and with a blocking layer (sol reaction time of 55 min, heat treatment temperature of 550 °C).

550 °C) was also recorded, and is given in Figure 8. The IPCE data for the DSC without a blocking layer were also recorded and are included in Figure 8 for comparison purposes. As Figure 8 shows the introduction of the TiO_2 blocking layer had no effect on the IPCE characteristics of the cell.

Thus, the unidirectional electron transport flow can be optimized by proper control of the interface contact at the molecular level, which can be helpful in the design and fabrication of DSCs with high overall cell conversion efficiency.

Conclusions

The formation of a dense TiO_2 blocking layer between the electrolyte and TCO surface by the sol-gel method enhanced the performance of the DSC. The sol-gel method resulted in the formation of a TiO_2 blocking layer with a smaller particle size, which was more efficiently packed onto the TCO substrate surface. This reduced the size of the voids present among the particles, which reduced the percolation of the electrolyte onto the FTO glass. The best cell performance was obtained for the cell with a TiO_2 blocking layer prepared with a sol reaction time of 55 minutes and heat-treated at 550 °C. The introduction of the blocking layer enhanced the overall conversion efficiency of the cell from 7.37 to 8.55%, an increase of 16%. The short-circuit current density and open-circuit voltage also showed an increase with the addition of a dense TiO_2 blocking layer, due to a decrease in the recombination rate at the TCO/electrolyte interface. Thus the overall conversion efficiency of the DSC can be further improved by optimizing the blocking layer.

Acknowledgments. This work was supported by the New Renewable Energy R&D Program of the Korea Institute of Energy Technology Evaluation and Planning (KETEP) grant funded by Korea government Ministry of Knowledge Economy [20093020010100].

References

1. O'Regan, B.; Gratzel, M. *Nature* **1991**, *353*, 737.
2. Nazeeruddin, M. K.; Kay, A.; Rodicio, I.; Humpbry-Baker, R.; Muller, E.; Liska, P.; Vlachopoulos, N.; Gratzel, M. *J. Am. Chem. Soc*. **1993**, *115*, 6382.
3. Ito, S.; Murakami, T. N.; Comte, P.; Liska, P.; Gratzel, C.; Nazeeruddin, M. K.; Gratzel, M. *Thin Solid Films* **2008**, *516*, 4613-4619.
4. Pelet, S.; Moser, J. E.; Gratzel, M. *J. Phys. Chem. B* **2000**, *104*, 1791-1795.
5. Rehm, J. M.; McLendon, G. L.; Nagasawa, Y.; Yoshihara, K.; Moser, J.; Gratzel, M. *J. Phys. Chem.* **1996**, *100*, 2820.
6. Xia, J.; Masaki, N.; Jiang, K.; Yanagida, S. *J. Photochem. and Photobiol. A: Chemistry* **2007**, *188*, 120-127.
7. Xia, J.; Yanagida, S. *Solar Energy doi:10.1016/j.solener.* **2009**, *10*, 005.
8. Hattori, R.; Goto, H. *Thin Solid Films* **2007**, *515*, 8045-8049.
9. Patrocinio, A. O. T.; Paterno, L. G.; Iha, N. Y. M. *J. Photochem. and Photobiol. A: Chemistry* **2009**, *205*, 23-27.
10. Cameron, P. J.; Peter, L. M. *J. Phys. Chem. B* **2003**, *107*, 14394-14400.
11. Hu, L. H.; Dai, S. Y.; Wang, J.; Xiao, S. F.; Sui, Y. F.; Huang, Y.; Chen, S. H.; Kong, F. T.; Pan, X.; Liang, L. Y.; Wang, K. J. *J. Phys. Chem. B* **2007**, *111*, 358-362.
12. Xia, J. B.; Masaki, N.; Jiang, K. J.; Yanagida, S. *J. Phys. Chem. C* **2007**, *111*, 8092-8097.
13. Gregg, B. A.; Pichot, F.; Ferrere, S.; Fields, C. L. *J. Phys. Chem. B* **2001**, *105*, 1422.
14. Xia, J. B.; Masaki, N.; Jiang, K. J.; Wada, Y.; Yamagida, S. *Chem. Lett.* **2006**, *35*, 252.
15. Waita, S. M.; Aduda, B. O.; Mwabora, J. M.; Niklasson, G. A.; Granqvist, C. G.; Boschloo, G. *J. Electroanal. Chem*. **2009**, *637*, 79-83.
16. Pechini, M. *US patent no. 3*. **1967**, *330*, 697.
17. Han, C.-H.; Lee, H.-S.; Han, S.-D. *Bull. Korean Chem. Soc.* **2008**, *29*, 1495.
18. Ferber, J.; Stangi, R.; Luther, J. *Sol. Energ. Mater. Sol. Cells* **1998**, *53*, 29-54.
19. Peter, L. *J. Electroanal. Chem*. **2007**, *599*, 233-240.
20. Hart, J. N.; Menzies, D.; Cheng, Y. B.; Simon, G. P.; Spiccia, L. *C. R. Chimie* **2006**, *9*, 622-626.